HEFAT2014
10th International Conference on Heat Transfer, Fluid Mechanics and Thermodynamics
14 – 16 July 2014
Orlando, Florida

IDENTIFICATION OF FLOW BOILING PATTERNS IN MINICHANNEL WITH THE USE OF ANALYSIS OF PRESSURE OSCILLATIONS

Grzybowski H., Mosdorf R.*
*Author for correspondence
Department of Mechanics and Applied Computer Science, Faculty of Mechanical Engineering,
Bialystok University of Technology,
Wiejska 45 C, 15-351 Bialystok,
Poland,
E-mail: r.mosdorf@pb.edu.pl

ABSTRACT

The dynamics of pressure fluctuations occurring in flow boiling in a minichannel with diameter of 1 mm, which consists of the heated section and glass condenser has been experimentally investigated and analysed. The recurrence plot and PCA of recurrence plot quantities have been applied. High speed digital video camera has been used to identify two-phase flow patterns in the glass condenser. The low frequency pressure fluctuations with relatively high amplitude which are caused by presence of compressible volume in the system have been observed. These fluctuations are accompanied by high frequency pressure oscillations. It has been found that during those fluctuations the dominant frequency of pressure fluctuations changes chaotically in time. Such pressure oscillations are accompanied by the flow patterns changes in the condenser. In the paper the new method of two-phase flow identification has been presented. The method is based on the analysis of dynamics of signal recorded from the pressure sensor. It has been shown that in the plots of two first components the points are grouped in the six separated clusters, which correspond to different flow patterns.

INTRODUCTION

Two-phase flow boiling instabilities are present in every heat exchanging system equipped in small diameter channel. Instabilities are associated with formation of isolated bubbles, confined bubbles, slugs, bubbly and annular flow patterns [1,2]. Brutin et al. [3] carried out the simultaneous visualization and measurement investigations of flow boiling of water in rectangular minichannels with a hydraulic diameter of 889 μm. They reported steady and unsteady thermo-hydraulic behaviours of flow boiling. The visualisations of vapour slug formation and reverse flow inside the minichannel have been made. The findings show that the rapid growth of bubbles causes the reverse flow. In the paper [4], the liquid film dryout was observed during the rapid evaporation of the liquid from channel walls. In a mini scale, the boiling becomes more unstable [5] in comparison with the boiling in normal size channels.

NOMENCLATURE

DET	[-]	Determinism
I	[-]	Generalised mutual information
l	[-]	Length of a diagonal line
m	[-]	Embedding dimension
n,N	[-]	Number of samples
$p(\cdot)$	[-]	Probability
p	[Pa]	Pressure
P	[W]	Power
$P(l)$	[-]	Probability to find a diagonal line of length l in the RP
$R_{i,j}$	[-]	Recurrence point
RR	[-]	Recurrence rate
t	[s]	Time
T	[K]	Temperature
x	[-]	Measured quantity

Special characters

τ	[-]	Time delay
ε	[-]	Radius of neighborhood (threshold for RP computation)
Θ	[-]	Heaviside function

Subscripts

min	Minimum
i,j	Point number

Therefore, the minichannel heat exchangers are more prone to different types of instabilities. The review of instabilities of two-phase flow in the minichannel have been presented in papers [6,7]. Kakac et al. [8] extensively investigated oscillations of flow rate and pressure in different types of minichannels. Four types of oscillations have been classified: pressure-drop oscillations, density-wave oscillations, acoustic oscillations and thermal oscillations. Long term oscillations generally called “pressure-drop type oscillations” were first

discussed by Stenning in his works [9,10,11]. The review of pressure drop type oscillations has been presented in the paper [12]. Padki et al. [13] classified pressure-drop oscillations and the Ledinegg instability using the bifurcation theory. Bargles et al. [14] noted that pressure drop oscillations occur, when the compressible volume upstream of the boiling channel exists and the channel pressure drop decreases together with increasing the mass flow rate in the negative-slope flow region. The mechanism of local vapour slug formation in confined geometry of minichannel has been discussed in the paper [15, 116]. A single minichannel, which is heated and cooled is called the pulsating heat pipe (PHP) [17,18]. The flow pulsations inside the minichannel are caused by interactions between the condensation and boiling which appear in the pipe. Yanxi Song, Jinliang Xu, [19] reported the appearance of chaotic behaviour of pulsating heat pipes systems.

The main aim of the present study was identification of flow boiling patterns in the minichannel by analysis of pressure oscillations. The minichannel of 1 mm inner diameter installed in the open loop with the compressible volume has been investigated. The experimental setup was designed in such a way that during the flow boiling the temperature fluctuations and pressure fluctuations occur. Additionally, the presence of boiling and condensation in the same minichannel also generate the flow oscillations. A high speed camera has been used to identify two-phase flow patterns in the glass minichannel installed in the outlet of the heated channel (condenser). For data analysis, there has been used recurrence plots and principal component analysis.

EXPERIMENTAL SETUP

Schematic diagram of the boiling system has been shown in Figure 1. The detail description of experimental stand is presented in [20]. Distilled water was pushed out from a supply tank (7 - Figure 1) by the compressed air. The ball valve, (8 - Figure 1), was used to regulate the liquid flow rate. It was setup in such a way that the liquid flow rate was 7.5 ml/min ± 0.5 ml/min. The heated section was made of a single circular brass pipe with inner diameter of 1 mm, outer diameter of 2 mm and length of 150 mm. The heat was supplied to the pipe on the length of 100 mm. The pipe was installed in the copper block with dimensions of 25x9x100 mm, shown in Figure 1. The outlet of brass pipe (length 25 mm)–was isolated and the thermocouple (type K with a diameter of 0.081 mm), (15 – Figure 1), was placed in the distance of 10 mm from the pipe outlet, as it is shown in Fig.1. The inlet water temperature was 19.1°C. The outlet pressure was the atmospheric pressure. The outlet of brass pipe was connected to the glass pipe (length of 150 mm, inner diameter of 1 mm and outer diameter of 5.7 mm), which allowed us to visualize the flow patterns (condenser). The outlet of the glass condenser was connected to the overflow tank (18 - Figure 1). Flow patterns were recorded with using the Casio EX-F1 digital camera at 1200 fps (336 x 96 pixels). Pressure difference between the brass pipe inlet and glass pipe outlet was measured using the silicon pressure sensor MPX12DP. The amount of vapour flowing through the glass pipe was measured by two laser-phototransistor sensors spaced 120 mm. Data from sensors was acquired by the acquisition system (Data translation 9804, 10 – Figure 1) at a sampling rate of 1 kHz.

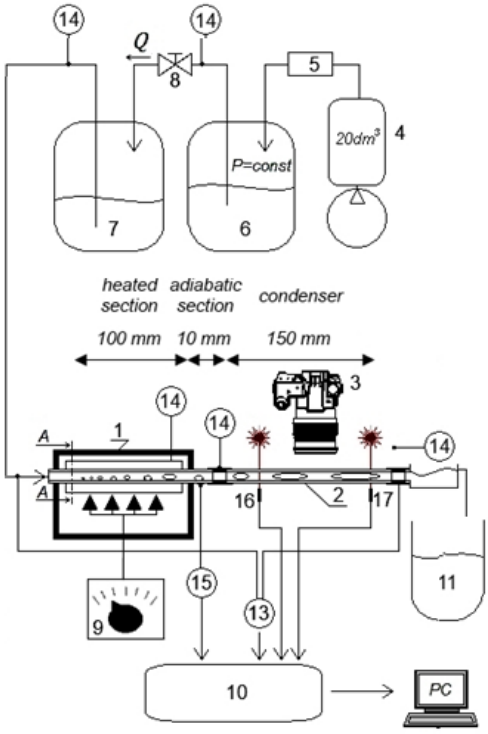

Figure 1 Schematic diagram of the experimental setup. 1 - heated section, 2 - glass tube, 3 - high speed camera, Casio EX-F1, 4 - air compressor, 5 - proportional pressure regulator, Metal Work Regtronic, 6 - supply tank, 5 dm3, 7 - surge tank of 5 dm^3, 8 - ball valve, 9 - power control, 10 - data acquisition system, data translation 9804, 11 - tank, 12 - PC, 13 - pressure sensor, MPX12DP, 14 - temperature sensor DS18B20, 15 - thermocouple, 16 - laser - phototransistor sensor 1, 17 - laser - phototransistor sensor 2, 18 – overflow tank.

The mechanism of appearance of pressure oscillations was as follows. Because the surge tank was airtight, therefore, the air pressure over the water surface in the surge tank (7 - Figure 1) depended on the amount of liquid in the tank. Therefore, the liquid level inside the surge tank was a function of the mutual relationship between the liquid flux supplied to the surge tank and the liquid flux flowing to the minichannel. The liquid flux flowing in the minichannel is a function of boiling and condensation. The gas compression in the surge tank induces the appearance of the pressure oscillations with low frequency. The temperature and pressure oscillations with high frequency observed in the experiment are caused by confined geometry of minichannel and have been previously discussed and modelled in the papers [13, 14, 20].

Figure 2 shows the examples of low and high frequency pressure fluctuations occurring in the system under consideration. Pressure fluctuations occurring with low frequency (Figure 2a) have a quasi periodic character. The low frequency fluctuations are the pressure drop type oscillations. Pressure fluctuations occurring with high frequency have a

chaotic character. In Figure 2b, the high frequency of pressure fluctuations in the single cycle of low frequency pressure fluctuations has been shown. These fluctuations are accompanied by appearance and disappearance of the slug and annular flow in the outlet of the heated minichannel.

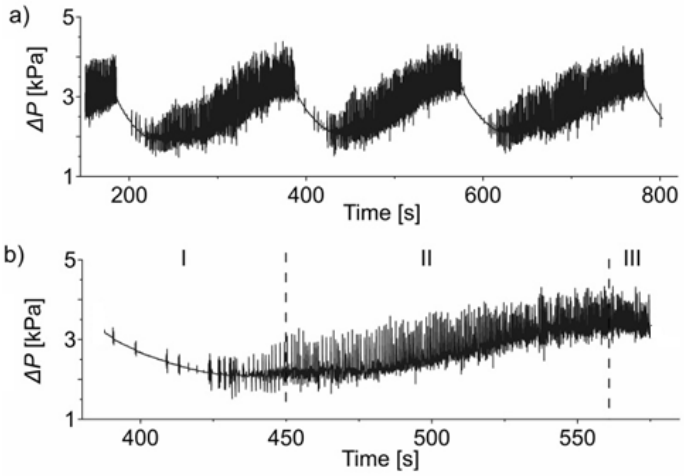

Figure 2 Plots of pressure fluctuations during two-phase flow boiling of water in minichannel. a) long reading with periodic boiling b) detailed view of single cycle of pressure fluctuation (P=46W).

In Figure 3b the three flow boiling modes have been marked. In the Figure 3, 4 and 5 the frames from recorded videos showing the flow patterns observed in each mode have been presented. The arrows located in the right side of frames indicate the flow direction.

At the beginning of the first mode (388 s) the channel is mainly filled with the liquid (Figure 3a). At 390 s, the first small pressure fluctuation can be observed which indicates that boiling occurs inside the channel and small vapour bubbles are visible in the glass channel outlet (Figure 3b). Next, the larger vapour bubbles (Figure 3c) and vapour slugs are visible in the glass condenser (Figure 3d). This kind of flow patterns is observed until 450 s. During the first mode, the average pressure decreases. Then, the sequence of flow patterns shown in Figure 3 is repeated. The frequency of occurrence of these sequence increases during the time.

The second mode starts at 450 s. In this mode the average pressure increases. Vapour slugs which grow inside the heated section are visible in the condenser (Figure 4a). Slugs condensate and shrinks (Figure 4b), the front of slug moves to the left side which is marked with the arrow. The condensed slug is being pushed out from the heated section and the flow in the right direction is established again (Figure 4c). After slugs, the bubbly flow is observed (Figure 4d). The sequence of flow patterns is repeated. The frequency of occurrence of this sequence increases during the time.

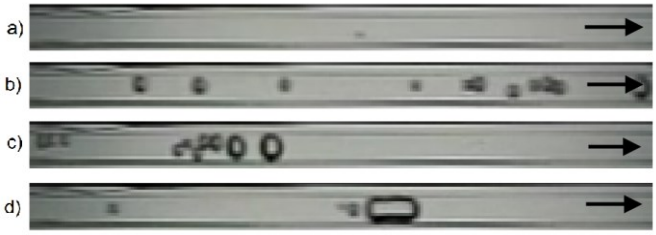

Figure 4 Sequence of flow patterns observed during the first mode. a) liquid flow, b) liquid flow with small vapour bubbles, c) liquid flow with vapour bubbles d) vapour slugs.

Figure 4 Sequence of flow patterns observed during the second mode. a) vapour flow, b) reversing long vapour slug, c) short vapour slugs with small vapour bubbles, d) bubbly flow.

The third mode starts at 560 s. During this mode, the channel is mainly filled with a vapour (Figure 5a). In Figure 5b,c the slug breakup has been shown. During this mode, the average pressure drop reaches the maximum.

Figure 5 Sequence of flow patterns observed during third mode. a) vapour flow, b) vapour flow with visible tearing areas, c) intermittent vapour flow

NON-LINEAR DATA ANALYSIS

The analysis of attractor of non-linear dynamical system gives us information about the properties of the system such as system complexity and its stability. In non-linear analysis the reconstruction of attractor in certain embedding dimension is carried out using the stroboscope coordination. The subsequent co-ordinates of attractor points are as follows.

$$\{x(t), x(t+\tau), ..., x[t+(n-1)\cdot\tau]\} \quad (1)$$

where x is a measured quantity.

In Figure 6 it has been show the 3D attractor reconstruction from pressure fluctuation occurring in the second mode (Figure 2b).

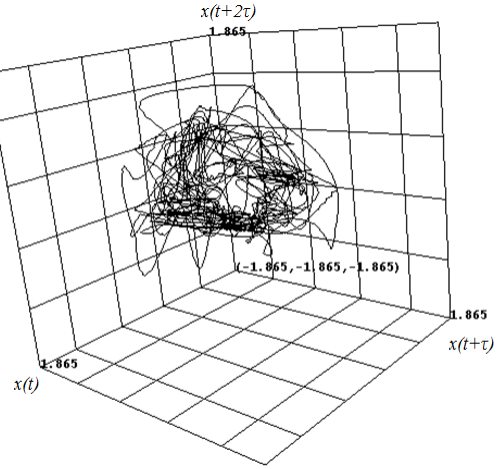

Figure 6 The attractor reconstruction for time series of the pressure drop fluctuations inside the minichannel for $\tau = 100$.

The image of the attractor in n-dimensional space depends on the time delay - τ. The mutual information between time series: $x(t)$ and $x(t+\tau)$ can be used to determine proper time delay for the reconstruction of attractors. As τ is increased, the mutual information decreases and then it rises again. The time delay for which the mutual information obtains the first minimum is a proper value of τ. The mutual information of $x(t)$ and $x(t+\tau)$ can be defined as [21]:

$$I(x(t),x(t+\tau))=\sum_{x(t+\tau)}\sum_{(x(t)}p[x(t),x(t+\tau)]\times \times\log_2\left\{\frac{p[x(t),x(t+\tau)]}{p[x(t)]p[x(t+\tau)]}\right\} \quad (2)$$

where $p[x(t),x(t+\tau)]$ is the joint probability distribution function of $x(t)$ and $x(t+\tau)$, and $p[x(t)]$ and $p[x(t+\tau)]$ are the marginal probability distribution functions of x and $x(t+\tau)$.The mutual information is equal to zero if $x(t)$ and $x(t+\tau)$ are independent random variables.

In Figure 7 it has been shown the mutual information functions vs time delay (number of samples) for the time series of pressure fluctuations occurring in the second mode (Figure 2b). For the time series of pressure fluctuations the first minimum is reached for time delay (number of samples) equal to 100. This value of time delay has been used for the attractor reconstruction, which is presented in Figure 6.

The false nearest neighbour algorithm has been used for the estimation of the proper embedding dimension of attractors. In this method, the changes of number of neighbours of points in embedding space with increasing embedding dimension are examined. The number of false neighbours is calculated for the whole time series under considerations and for several dimensions until the percent of false points reaches zero. Such dimension is treated as a proper embedding dimension for attractor reconstruction. In Figure 8 it has been shown the changes of the number of false neighbours vs the embedding dimension. Results show that 3D attractor reconstruction shown in Figure 6 is proper for time series which are examined.

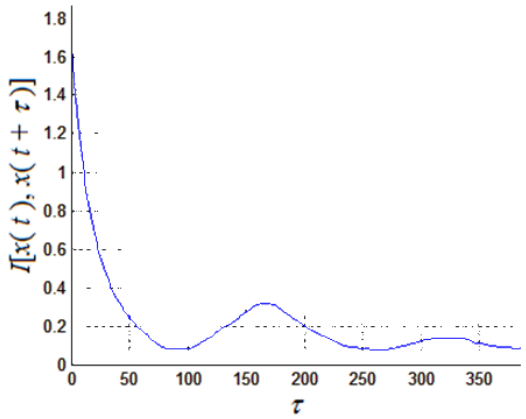

Figure 7 The mutual information functions vs time delay (number of samples) for the time series recorded from pressure sensors. The calculations have been made using the Matlab Toolbox [22].

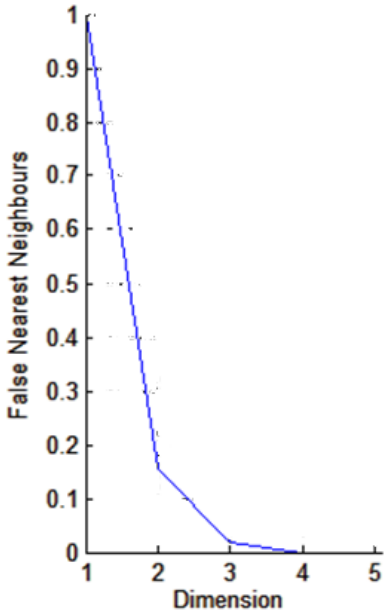

Figure 8 The changes of number of false nearest neighbours points for the pressure oscillations in the second mode (Figure 2b), P = 46W. The calculations have been made using the Matlab Toolbox [22].

Recurrence plot

Recurrence plot is a technique of visualization of the recurrence of states x_i in m-dimensional phase space. The recurrence of states at time i and at a different time j is marked with black dots in the 2D plot, where both axes are time axes. The recurrence plot is defined as [21]:

$$R_{i,j}=\Theta(\varepsilon - \|x_i - x_j\|), x_i \in \Re^m, i,j = 1...N \quad (3)$$

where N is the number of considered states x_i, ε_i is a threshold distance, $\|\ \|$ is a norm and Θ is the Heaviside function.

In Figure 9 it has been shown the recurrence plots of pressure fluctuations during the 10 s from different parts of the signals in the second mode (Figure 2b).

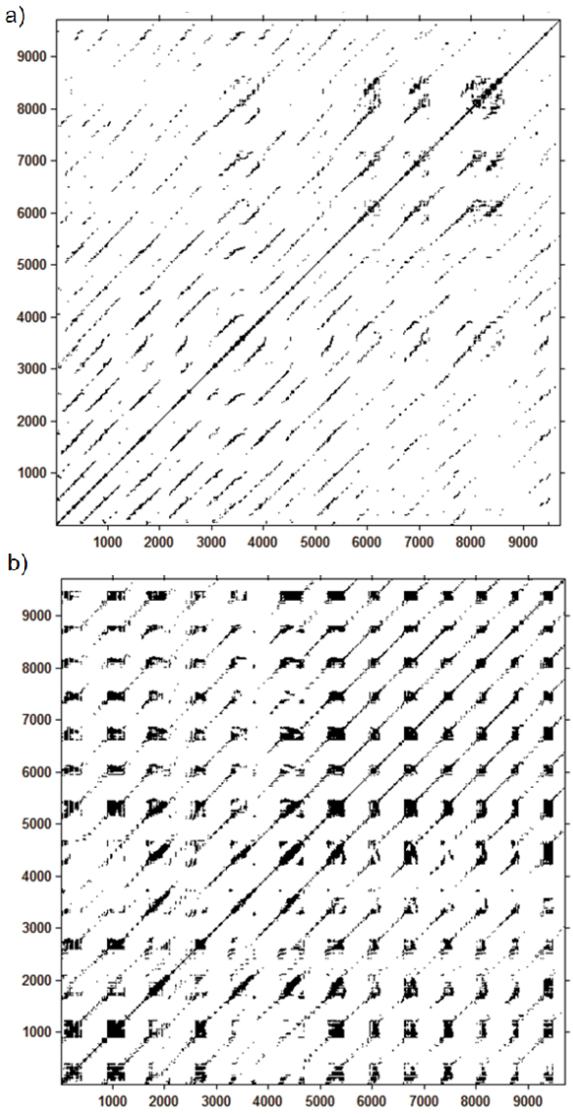

Figure 9 Recurrence plots for embedding dimension 4, time delay 100 and $\varepsilon = 0.8$. a) RP of signals from 530s to 540 s b) RP of signals from 480s to 490 s. The calculations have been made using the Matlab Toolbox [22].

In both recurrence plots, there are visible the diagonal structures. The distance between them indicates the time period between subsequent formations of slugs.

The recurrence rate, *RR,* is a measure of the percentage of recurrence points in the recurrence plot. It is defined as follows [21]:

$$RR = \frac{1}{N^2}\sum_{i,j'0}^{N} R_{i,j} \tag{4}$$

The value of *RR* corresponds to the correlation sum.

The number of points, which appear in the recurrence plot depends on the value of ε. The recurrence rate is a non-linear function of ε. In Figure 10 it is presented the function $RR(\varepsilon)$ obtained for time series under consideration. Strong nonlinearity of function $RR(\varepsilon)$ is visible for the small value of ε. For the higher value of ε the nonlinearity becomes smaller (the function becomes quasi linear). It has been assumed that the lowest value of ε in the linear part of function $RR(\varepsilon)$ is a proper value of ε for the reconstruction of recurrence plot. For time series under consideration it is equal to 0.8 (Figure 10).

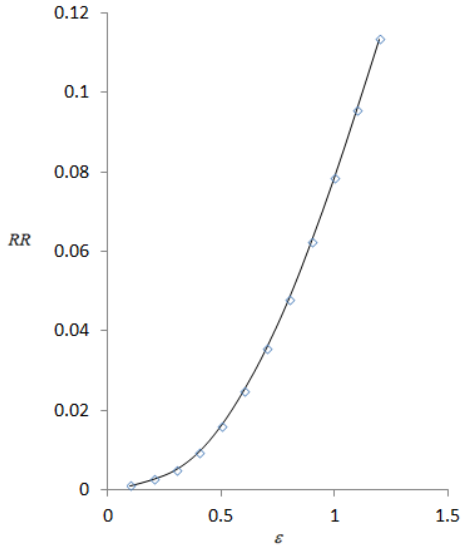

Figure 10 Recurrence rate (*RR)* vs ε for time series of pressure fluctuations (embedding dimension 4, $\varepsilon = 0.8$, $\tau = 100$). The calculations have been made using the Matlab Toolbox [22].

The determinism, *DET,* is defined as the percentage of black points which belong to diagonal lines of the length greater than l_{min}. It is defined as [21]:

$$DET = \frac{\sum_{l=l_{\min}}^{N} lP(l)}{\sum_{l=1}^{N} lP(l)} \tag{5}$$

where $P(l)$ denotes the probability of finding a diagonal line of length l in the RP.

For a periodic system, $DET = 1$ and for stochastic system *DET* tends to zero [21].

The average length of diagonal lines, *AVG*, is defined by the following relation [21]:

$$AVG = \frac{\sum_{l=l_{\min}}^{N} lP(l)}{\sum_{l=l_{\min}}^{N} P(l)} \tag{6}$$

Gao [23] defines the recurrence time of the first type T^1 and second time T^2. The recurrence time is calculated as the distance between points belonging to the vertical lines in RP. In case of recurrence time of the first type T^1, all points of RP are considered. Such value of T^1 depends on the trajectory density and value of ε. In case of recurrence time of the second type T^2 the vertical distances between the pairs "white" pixel/"black" pixel in the columns are measured [22]. Then, in this case for the periodic motion, the T^2 accurately estimates the period of the motion. This type of recurrence time is related to entropy and to the information dimension of the attractor [21, 22].

Windowed quantitative recurrence analysis

The pressure fluctuations were analysed with the use of the windowed quantitative recurrence analysis. The moving window was set to 5000 samples, window step to 1000 samples. The minimum length of diagonal and vertical lines was equal to 10 samples. Theiler window was equal to 1. The embedding dimension was 3 and a time delay was 100. The radius was equal to 0.8. The windowed quantitative recurrence analysis generates the time series of coefficients which show the changes in time of the dynamics of two-phase flow patterns.

The four time series ($DET(t)$, $AVG(t)$, $T^1(t)$, $T^2(t)$) have been analysed as a set of variables describing the dynamics of two phase flow patterns. These time series have been shown in Figure 11 and 12.

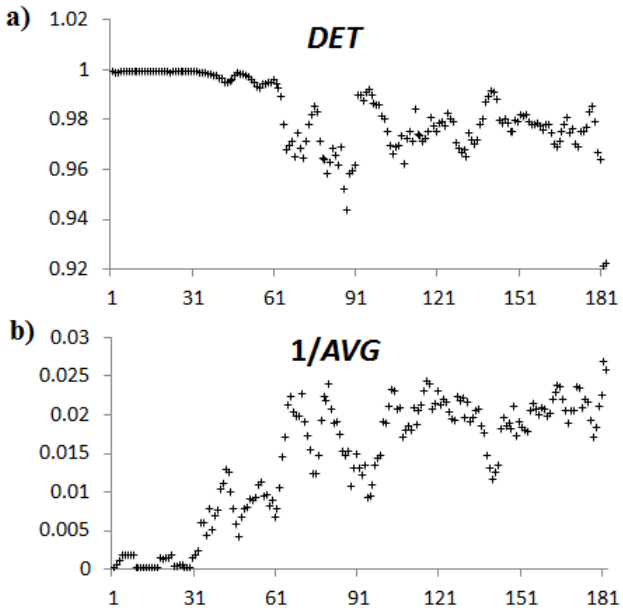

Figure 11 Changes in time of coefficients DET and $1/AVG$. a) DET, b) $1/AVG$. Embedding dimension 4, $\varepsilon = 0.8$, $\tau = 100$. The calculations have been made using the Matlab Toolbox [22].

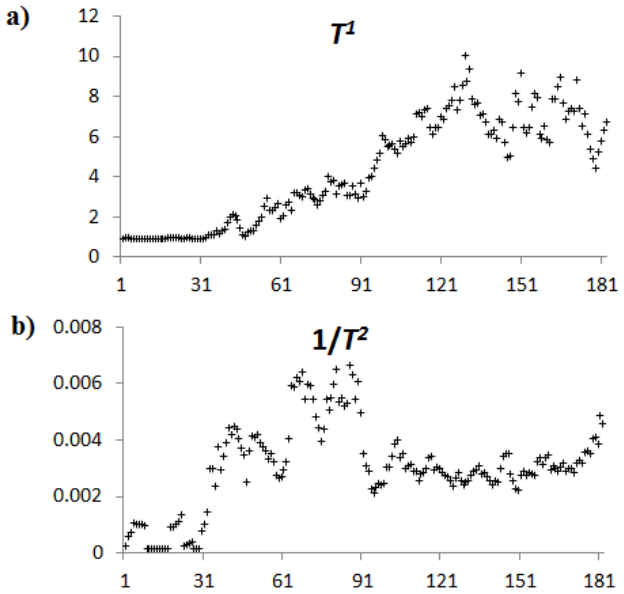

Figure 12 Changes in time of coefficients T^1 and $1/T^2$. a) T^1, b) $1/T^2$. Embedding dimension 4, $\varepsilon = 0.8$, $\tau = 100$. The calculations have been made using the Matlab Toolbox [22].

Principal component analysis

The coefficients generated by quantitative recurrence analysis describe the various aspects of dynamical system but they are correlated. Therefore, they cannot be treated as independent variables describing the system dynamics. For that reason, the principal component analysis (PCA) has been used to obtain the set of independent variables which, characterise the dynamics of system under consideration.

The principal component analysis is a method that uses the orthogonal transformation to convert an input set of data into a new set of data, in a new set of coordinates called the principal components. This transformation is defined in such a way that the data has the largest possible variance around the first principal component. For the successive components the variance of data decreases. An ordered eigenvalues of the covariance matrix - [DET, $1/AVG$, T^1, T^2] are shown in Fig.13.

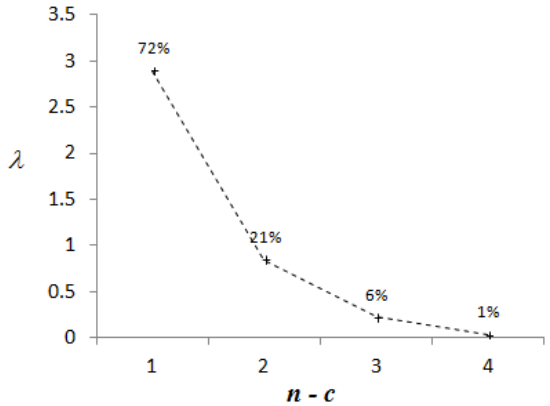

Figure 13 An ordered eigenvalues of the covariance matrix - [DET, $1/AVG$, T^1, T^2].

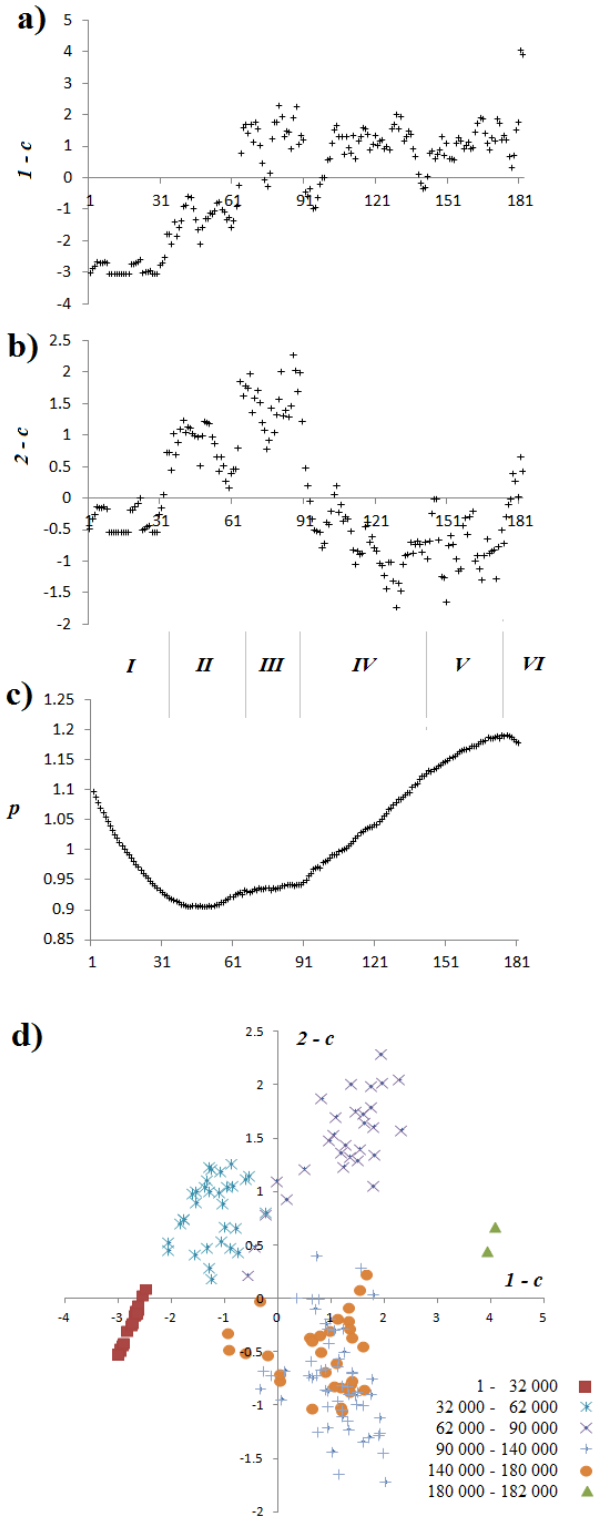

Figure 14 The changes of the first two components and average pressure drop. a) first component, b) second component, c) mean pressure drop, d) 2D map of different structures of two phase flow in the minichannel in the space of the first and second components.

Obtained results show that the first two components explain the 72% + 21% = 83% of input data variation. In Figure 14 it has been shown the plots of the first two components (Figure 14a,b), the average values of pressure changes (Figure 14c) and 2D map of different structures of two phase flow in the minichannel in the space of the first and second components (Figure 14d).

In the map (Figure 14) the points are grouped in the six different areas marked with successive numbers. The corresponding time periods are shown between the Figure 14b and Figure 14c.

CONCLUSION

In the paper the new method of two-phase flow identification has been presented. The method is based on the analysis of dynamics of signal recorded from the pressure sensor.

In the proposed method, the quantitative recurrence analysis uses the normalized signals, so the average values of the signal do not affect the results of the analysis. Despite of the neglect of quantitative signal characteristics, the qualitative analysis of its dynamics allows us for the identification of the two-phase flow patterns. It has been shown that in the plots of the two first components the points are grouped in the six separated clusters, which correspond to different flow patterns.

Obtained results confirm that this type of analysis can be used to identify the two-phase flow patterns in the minichannel. The final verification of the proposed method requires a much larger number of analyses of different types of two-phase flows.

Acknowledgement

The project was funded by the National Science Centre, Poland - the number of decision: DEC-2013/09/B/ST8/02850.

REFERENCES

[1] S.G. Kandlikar, Two-phase flow patterns, pressure drop, and heat transfer during boiling in minichannel flow passages of compact evaporators, *Heat Transfer Engineering* 23 (2002) 5-23

[2] D. Brutin, V.S. Ajaev, L. Tadrist, Pressure drop and void fraction during flow boiling in rectangular minichannels in weightlessness, *Applied Thermal Engineering* 51 (1–2) (2013) 1317-1327

[3] D. Brutin, F. Topin, L. Tadrist, Experimental study of unsteady convective boiling in heated minichannels, *International Journal of Heat and Mass Transfer* 46 (16) (2003) 2957-2965

[4] M. E. Steinke, S. G. Kandlikar, An Experimental Investigation of Flow Boiling Characteristics of Water in Parallel Microchannels, *Journal of Heat Transfer* 126 (4) (2004) 518-526

[5] S.G. Kandlikar, Fundamental issues related to flow boiling in minichannels and microchannels, *Experimental Thermal and Fluid Science* 26 (2–4) (2002) 389-407

[6] L. Tadrist, Review on two-phase flow instabilities in narrow spaces, *International Journal of Heat and Fluid Flow* 28 (1) (2007) 54-62

[7] S. Kakac, B. Bon, A Review of two-phase flow dynamic instabilities in tube boiling systems, *International Journal of Heat and Mass Transfer* 51 (3-4) (2008) 399-433
[8] S. Kakac, B. Bon, A Review of two-phase flow dynamic instabilities in tube boiling systems, International Journal of Heat and Mass Transfer 51 (3-4) (2008) 399-433
[9] A.H. Stenning, Instabilities in the flow of a boiling liquid, *J. Basic Eng. Trans.* ASME Ser. D (86) (1964) 213–228
[10] A.H. Stenning, T.N. Veziroglo, Flow oscillation modes in forced convection boiling, *Proceedings of the Heat Transfer and Fluid Mechanics Institute*, Stanford Univ. Press, (1965) 301–316
[11] A.H. Stenning, T.N. Veziroglo, G.M. Callahan, Pressure-drop oscillations in forced convection with boiling system, *Symposium on Two Phase Flow Dynamics*, Eindhoven, Netherlands, 1967, pp. 4-9
[12] E. Manavela Chiapero, M. Fernandino, C.A. Dorao, Review on pressure drop oscillations in boiling systems, *Nuclear Engineering and Design* 250 (2012) 436-447
[13] M. Padki, K. Palmer, S. Kakaç, T.N. Veziroğlu, Bifurcation analysis of pressure-drop oscillations and the Ledinegg instability, *International Journal of Heat and Mass Transfer* 35 (2) (1992) 525–532
[14] A.E. Bergles, J. H. Lienhard V, G.E. Kendall, P. Griffith, Boiling and Evaporation in Small Diameter Channels, *Heat Transfer Engineering* 24 (1) (2003) 18–40.
[15] D. Brutin, L. Tadrist, Destabilization mechanisms and scaling laws of convective boiling in a minichannel, *Journal of Thermophysics and Heat Transfer* 20 (4) (2006) 850-855
[16] J. Barber, D. Brutin, K. Sefiane, J.L. Gardarein, L. Tadrist, Unsteady-state fluctuations analysis during bubble growth in a "rectangular" microchannel, *International Journal of Heat and Mass Transfer* 54 (23-24) (2011) 4784-4795
[17] Jian Qu, Huiying Wu, Ping Cheng, Xiong Wang, Non-linear analyses of temperature oscillations in a closed-loop pulsating heat pipe, *International Journal of Heat and Mass Transfer* 52 (15–16) (2009) 3481-3489
[18] S.P. Das, V.S. Nikolayev, F. Lefevre, B. Pottier, S. Khandekar, J. Bonjour, Thermally induced two-phase oscillating flow inside a capillary tube, *International Journal of Heat and Mass Transfer* 53 (19–20) (2010) 3905-3913
[19] Yanxi Song, Jinliang Xu, Chaotic behavior of pulsating heat pipes, International *Journal of Heat and Mass Transfer* 52 (13–14) (2009) 2932-2941
[20] H. Grzybowski, R. Mosdorf, Dynamics of pressure oscillations in flow boiling and condensation in the minichannel, *International Journal of Heat and Mass Transfer*, 2014, accepted for publication, 10.1016/j.ijheatmasstransfer.2014.02.028
[21] N. Marwan , M. C. Romano, M. Thiel, J. Kurths, Recurrence Plots for the Analysis of Complex Systems, *Physics Reports*, 438(5-6), 237-329, 2007
[22] N. Marwan, Cross Recurrence Plot Toolbox for Matlab, Ver. 5.15, Release 28.10, http://tocsy.pik-potsdam.de
[23] J. Gao, J. Hu. Fast monitoring of epileptic seizures using recurrence time statistics of electroencephalography. *Front Comput Neurosci*. 2013; 7: 122. Published online 2013 October 1. doi: 10.3389/fncom.2013.00122